Thermoresponsive Conductive Polymer Composite Thin Film and Fiber Mat: Crosslinked PEDOT:PSS and P(NIPAAm-*co*-NMA) Composite

Shih-Ru Huang,[1] King-Fu Lin,[1,2] Trong-Ming Don,[3] Chai-Fen Lee,[4] Man-Sheng Wang,[5] Wen-Yen Chiu[1,2,6]

[1]Institute of Polymer Science and Engineering, National Taiwan University, Taipei, Taiwan
[2]Department of Materials Science and Engineering, National Taiwan University, Taipei, Taiwan
[3]Department of Chemical and Materials Engineering, Tamkang University, New Taipei City, Taiwan
[4]Department of Cosmetic Science, Chia Nan University of Pharmacy and Science, Tainan 71710, Taiwan
[5]Department of Chemical Engineering and Biotechnology, National Taipei University of Technology, Taipei, Taiwan
[6]Department of Chemical Engineering, National Taiwan University, Taipei, Taiwan
Correspondence to: W.-Y. Chiu (E-mail: ycchiu@ntu.edu.tw) and T.-M. Don (E-mail: tmdon@mail.tku.edu.tw)

Received 3 July 2015; accepted 28 August 2015; published online 28 October 2015
DOI: 10.1002/pola.27945

ABSTRACT: The thermoresponsive conductive composite (TCC) thin films and fiber mats, whose electrical property changed with temperature, were fabricated successfully. The thermocrosslinkable and thermoresponsive copolymer, poly (*N*-isopropyl acrylamide-*co*-*N*-methylolacrylamide) (PNN), was synthesized. The TCC thin film and fiber mat were fabricated by spin coating and electrospinning process of PEDOT:PSS/PNN solutions, respectively. After thermocrosslinking and doping by DMSO, the composite thin films and fiber mats were obtained. Fibrous structures of TCC fiber mats were observed by SEM. The surface resistance and conductivity of composites were measured. The thermoresponsivity and swelling ratio of TCCs were also studied. The thermoresponsive conductive property was analyzed by measuring the surface resistance of TCCs in water bath under various temperatures from 20 to 50 °C. With the increase of temperature, the TCCs shrank to be dense structure and showed lower surface resistance. The TCC fibers mat exhibited greater sensitivity to temperature than thin film owing to its fibrous structure. © 2015 Wiley Periodicals, Inc. J. Polym. Sci., Part A: Polym. Chem. **2016**, *54*, 1078–1087

KEYWORDS: composite; conductive polymer; thermo-responsive

INTRODUCTION Stimuli-responsive polymers which rapidly change their configuration, dimensions or physical properties with appropriate stimuli such as heat, pH value, electricity, magnetic field, light, and solvent have received more and more attention owing to their variety of applications especially in the biomedical field.[1,2] Poly-(*N*-isopropylacrylamide)(PNIPAAm) is a well-known thermoresponsive polymer which undergoes a reversible phase transition at the temperature which is called lower critical solution temperature (LCST) near 32 °C in aqueous solution.[3] By changing the temperature from below LCST to above LCST, PNIPAAm turns from hydrophilicity to hydrophobicity rapidly. This thermoresponsive behavior was intensively studied by researchers in the past few decades. In addition, PNIPAAm is a biocompatible material and LCST is near the temperature of human body, so PNIPAAm-based materials can be used in the biomedical field. For instance, IPN-PNIPAAm hydrogels are used for protein loading and release.[4,5]

One-dimensional composite fibers with low dimensions and large surface area attract more attention for their potential in novel functional material. Electrospinning process is a facile method to fabricate one-dimensional inorganic/polymer and polymer/polymer composite nanofibers which show plenty of functionalities originated from the materials.[6] Owing to their facility, low dimensions, and large surface area, electrospun composite fibers can be applied in many fields such as filters,[7] nanosensors,[8,9] tissue engineering,[10] wound dressing,[11] drug release, and so on. In other words, electrospinning process can enlarge the active surface area and improve the performance of composite. In addition, conductive polymer composite microfibers and nanofibers receive more attention in recent years, owing to their potential in plenty of applications, such as low power consumption devices, ultrasensitive sensors, and so on.[12–16]

To improve the stability and mechanical properties of electrospun fibers, the crosslinking technique is an important issue in recent research. Two effective methods to build

TABLE 1 Compositions of Solutions for Fabricating TCC Thin Films

Sample code	PNN (g)	PEDOT:PSS solution (g)	Water (g)	PEDOT:PSS content in the composite (wt %)
PNN-fm	0.05	0	0.95	0
PDPNN4-fm	0.05	0.15	0.8	3.8%
PDPNN8-fm	0.05	0.35	0.6	8.4%
PDPNN12-fm	0.05	0.55	0.4	12.6%
PDPNN16-fm	0.05	0.75	0.2	16.4%
PDPNN20-fm	0.05	0.95	0	19.9%

chemical crosslinking in electrospun fibers are condensation and radical polymerization. Both of them generate new chemical bonds among polymer chains by postcuring process. Some polymers with functional groups such as hydroxyl, carboxylic acid groups and so on, can react by condensation reaction after thermocuring.[17,18] On the other hand, polymers with C═C double-bonds, such as polybutadiene, can polymerize by UV curing.[19,20] Moreover, crosslinking agents containing multifunctionality can be also applied to crosslink electrospun fibers.[21–23] The development of crosslinking technique not only improves the stability of fiber mat but also expands the application fields.

Conductive polymer composite fibers were investigated intensively by researchers in recently years, however, few researchers focused on the combination of thermoresponsive and conductive polymers that might have potential in sensor application. In this study, thermoresponsive conductive composite (TCC) thin films and fiber mats were fabricated successfully. Fiber mats with high porosity and large active area showed different thermoresponsive and conductive properties compared to thin films. In order to crosslink polymer composite, thermocrosslinkable monomer NMA was copolymerized with NIPAAm to synthesize thermocrosslinkable copolymer (poly-(*N*-isopropylacrylamide-*co*-*N*-methylolacrylamide)) (PNN). TCC fiber mats and thin films containing conductive poly(3,4-ethylenedioxythiophene): polystyrene sulfonate (PEDOT:PSS) and PNN were fabricated by electrospinning and spin-coating process, respectively. After thermocrosslinking process, stable TCCs were obtained. Structure of TCC fibers were observed by SEM. Thermoresponsivity and conductive properties of TCCs were also studied. Thermodependent conductive property of TCCs was measured by detecting surface resistance under various temperatures. In this test, surface resistance change of TCC fiber mats was greater than that of thin films. In other word, TCC fiber mats exhibited better thermodependent conductive property than thin films.

EXPERIMENTAL

Materials

N-isopropylacrylamide (NIPAAm; Acros), ammonium persulfate (APS; Acros), sodium metabisulfite (SMBS; Acros), *N*-(hydroxymethyl) acrylamide (NMA; 48 wt % in water; Aldrich), poly(3,4-ethylenedioxythiophene): polystyrene sulfonate aqueous solution (PEDOT:PSS 1.31 wt %; Sigma-Aldrich), Dioctyl sulfosuccinate sodium salt (AOT; Sigma-Aldrich) silver paste (Gredmann), HCl (37 wt % in water; Scharlau), deuterium oxide (D_2O; Aldrich) were used as supplied. Distilled and deionized water was used throughout the work.

Sample Preparation

Synthesis of Crosslinkable Thermoresponsive Copolymer

Poly(*N*-isopropylacrylamide-*co*-*N*-methylol acrylamide) (PNN) was synthesized using redox initiation polymerization in aqueous solution. First, 2.6 g of NIPAAm and 0.42 mL of NMA were dissolved in 20.2 mL of water. Then, 0.027 g of APS and 0.0226 g of SMBS, which were dissolved in 0.4 mL of water respectively, were added into the above solution with stirring. The solution was later placed in the water bath stationarily at 26 °C for one day for the reaction. After polymerization, the gel-like product was dissolved in 12 mL of HCl solution. Then, this acidic PNN solution was dialyzed for 3 days until the pH value was greater than 5. Finally, the PNN solution was freeze-dried to obtain the PNN powder.

Fabrication of PDPNN Thin Films

PDPNN was the acronym of the combination of PEDOT:PSS and PNN, and their thin films were fabricated by spin coating. First, adequate amount of PEDOT:PSS, PNN and water were mixed and stirred for 12 h to obtain homogeneous PDPNN solutions. The compositions and PEDOT:PSS contents in the composites were arranged in Table 1. Then, 0.3 mL of PDPNN solutions were dropped on the glass substrates and spin coating process was carried out at 1200 rpm for 10 s. Later, the PDPNN thin films were put into oven for thermocrosslinking at 110 °C for 12 h. Finally, PDPNN thin films were fabricated for further processing.

Fabrication of PDPNN Fiber Mats

PDPNN fiber mats mainly composed of PEDOT:PSS and PNN were prepared by electrospinning process. First, adequate amount of PEDOT:PSS, PNN, AOT, and water were mixed and stirred for 12 h to obtain homogeneous PDPNN solutions. The compositions and PEDOT:PSS contents in the composites were arranged in Table 2. Second, the PDPNN solutions were electrospun to PDPNN fiber mats. In the electrospinning, the composite solutions were loaded in the syringe which was pushed forward by pump with the injection rate of 0.1 mL/

TABLE 2 Compositions of Electrospinning Solutions for Fabricating TCC Fiber Mats

Sample code	PNN (g)	PEDOT:PSS solution (g)	Water (g)	AOT (g)	PEDOT:PSS Content in the Composite (wt %)	Solid Content (wt %)
PNN-fb	0.16	0	1.84	0.02	0	8%
PDPNN4-fb	0.154	0.462	1.384	0.02	3.8%	8%
PDPNN8-fb	0.146	1.026	0.826	0.02	8.4%	8%
PDPNN12-fb	0.14	1.538	0.321	0.02	12.6%	8%
PDPNN16-fb	0.125	1.875	0	0.02	16.4%	7.5%
PDPNN20-fb	0.1	1.9	0	0.02	19.9%	6.2%

h. The distance between point of the needle and conductive collector was 12.5 cm. The composite solutions were electrospun at the voltage of 20 kV for 30 min to fabricate PDPNN fiber mats. After thermocrosslinking at 110 °C for 12 h, the composite fiber mats were obtained for further processing.

Doping and Shaping of TCC Electrode

In order to increase the conductivity of PEDOT:PSS in TCCs, the doping process was applied on the PDPNN thin films and fiber mats. In the doping process, the composite thin films and fiber mats were immersed in DMSO for 10 min.[24] Second, they were dried in the oven at 110 °C. Later, they were shaped to be 1 cm in width. Next, silver paste was applied cross the composite thin films and fiber mats to form two parallel silver electrodes. After drying the silver paste at 110 °C, the thermoresponsive conductive composite thin films and fiber mats with 1 × 1 cm^2 active area were fabricated. The diagram of TCC sensor was shown in Figure 1.

Characterization

NMR Analysis of PNN

To identify the NMA content in the copolymer PNN, ^1H nuclear magnetic resonance (NMR) spectroscopy was carried out with BRUKER AVANCE 500MHz NMR to characterize the chemical structure at room temperature. 1 wt % of PNN dissolved in D_2O was prepared for NMR analysis.

GPC Analysis of PNN

Molecular weight distribution of the copolymer PNN was measured by gel permeation chromatography (Shodex RI SE-61) system equipped with refractive index detector. THF was used as the eluent at a flow rate of 1 cm^3/min. The copolymer PNN powder was dissolved in THF at a concentration of 1 mg/cm^3. Narrow MWD polystyrene standards with molecular weights ranging from 580 to 377,400 g/mol were used for calibration.

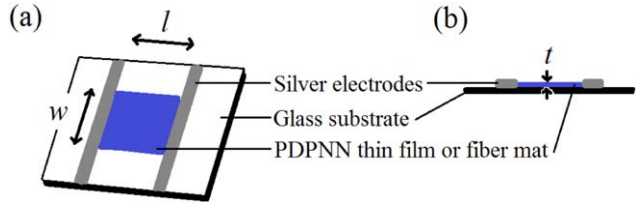

FIGURE 1 Schematic diagram of TCC electrode: (a) top view, (b) cross-section view. [Color figure can be viewed in the online issue, which is available at wileyonlinelibrary.com.]

Gel Fraction and Swelling Ratio

To study the stability of TCCs, the gel fractions of stable samples were measured. The weights of composites after thermocrosslinking were recorded and denoted as Wo. Subsequently, the composites were immersed in water for 1 day and dried in the oven; the weights of dried composites were measured and denoted as Wd. The gel fractions were calculated using eq 1.

$$\text{Gel fraction} = \text{Wd}/\text{Wo} \quad (1)$$

The measurement of swelling ratio is a way to know the water-absorption ability as well as thermoresponsivity of material. In the experiment, crosslinked TCC films, which were formed in the Teflon mold, and fiber mats were soaked in the water with different temperatures from 25 to 50 °C for 3 min. Then, composite sample were filtered by a 300-mesh metal filter to remove excess water on the surface. Subsequently, the total weights of these swollen samples were measured and denoted as Ws. Finally, the swelling ratio defined as eq 2 was obtained.

$$\text{Swelling ratio} = \text{Ws}/\text{Wd} \quad (2)$$

Thermal Analysis

The phase transition behavior (LCST) of TCC films and fiber mats were measured by DSC (Perkin-Elmer Pyris 6). Crosslinked TCC films and fiber mats which absorbed water were put in the aluminium pan. The samples were heated from 25 to 45 °C at the rate of 2 °C/min.

Morphological Analysis

For observing the morphology of PNN fiber mats by SEM (JEOL JSM-6700F), the swollen-dried and shrunk-dried PNN, PDPNN-4, PDPNN-12, and PDPNN-20 fibers mats were fabricated. The composite fiber mats were immersed in water, then freeze-dried, dried at room temperature (below LCST), and dried in the oven at 50 °C (above LCST) to fabricate the swollen-dried and shrunk-dried samples, respectively.

Conductivity and Surface Resistance

For measuring electrical properties of TCCs, the surface resistance (R), and thickness (t) of TCC electrode with 1 ×

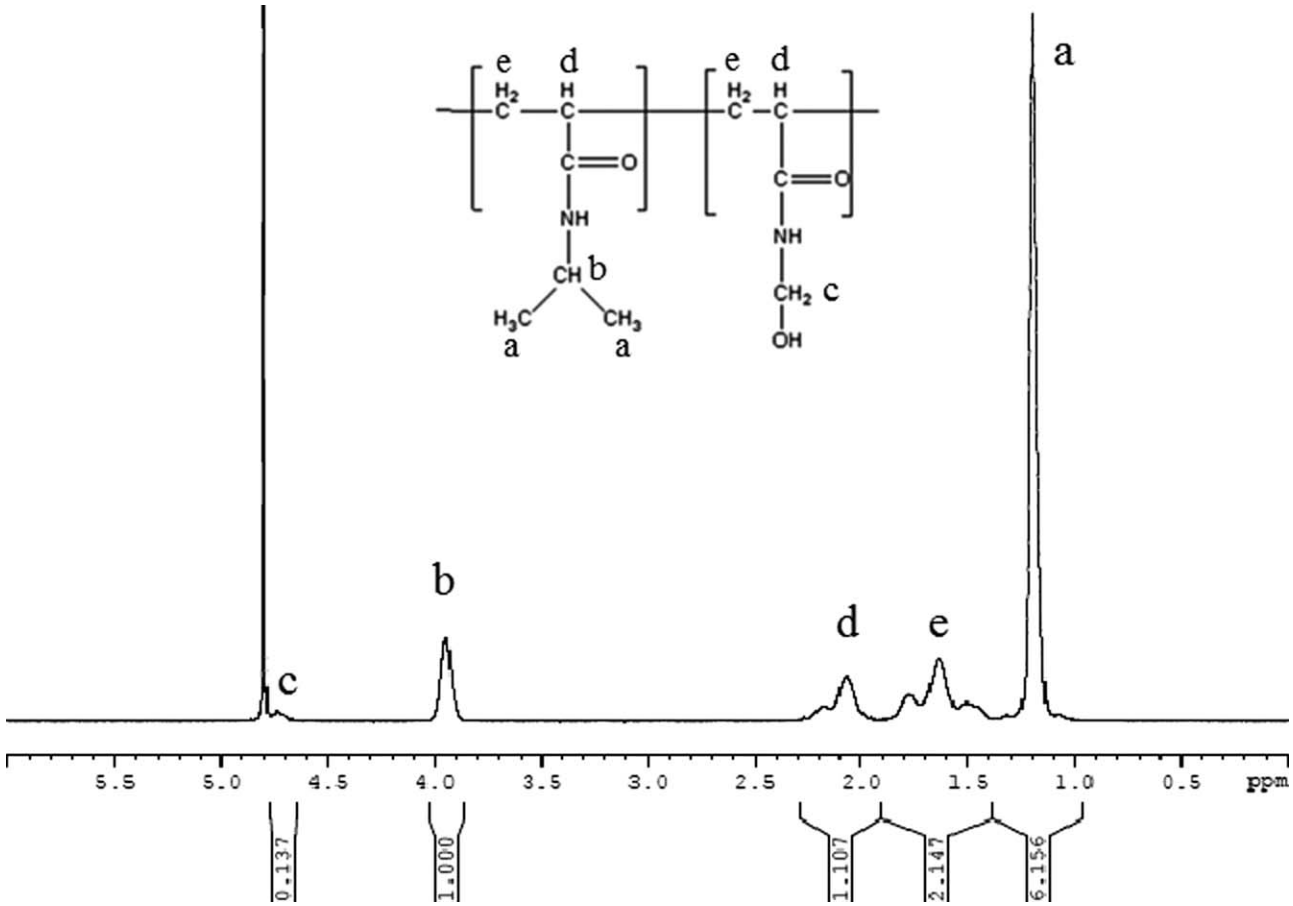

FIGURE 2 NMR spectrum of copolymer PNN.

1 cm^2 area were measured by voltmeter and α-step, respectively. The definition of conductivity (σ) is shown in eq 3.

$$\sigma = 1/(Rwt) = 1/(Rt) \quad (3)$$

where R, w, t, and l were surface resistance, width, thickness, and length of TCC electrode, respectively, as shown in Figure 1.

Thermoresponsive Conductive Property of TCC Electrode

The surface resistance change of TCC electrode with temperature was measured by electricity meter. First, TCC thin films and fiber mats were immersed in water bath at 25 °C. Next, by changing the temperature of water bath, the surface resistances of TCC sensors at different temperatures from 25 to 50 °C were measured.

RESULTS AND DISSCUSSION

Structural Characterization of PNN

To study the NMA content in the PNN copolymer, 1H NMR analysis was used. The chemical structure and NMR result were shown in Figure 2. The characteristic chemical shifts were also labeled corresponding to the specific protons. The molar ratio of NMA calculated by integration values of peaks *b*, *d*, and *e* was 7.8 mol % that was near the feeding ratio of NMA (8 mol %).

Molecular weight distribution and relative molecular weight of PNN were measured by GPC. The number average molecular weight (M_n) and weight average molecular weight (M_w) were 135,530 and 233,100 g/mol, respectively, and the PDI (M_w/M_n) was 1.52.

Electrospinning of PNN and PDPNN Fiber Mat

In the electrospinning process of PDPNN solutions, water which has high surface tension was chosen as the solvent because of its good solubility of PEDOT:PSS and PNN. However, electrospinning solution with high surface tension always generates the beaded fibers or drops that affected morphology and performance of product. Several researches showed that adding surfactant in the electrospinning solution can effectively decrease surface tension so as to prepare fiber with smooth surface.[25,26] In this study, to obtain electrospinning solution with low surface tension, 1 wt % of anionic surfactant, AOT, was mixed in the PDPNN solutions. The composition and surface tension of electrospinning solutions were shown in Tables 2 and 3, respectively. In Table 3, after adding 1 wt % of AOT, the surface tensions of all electrospinning solutions decreased near 30 mN/m and those were low enough to carry on electrospinning process. But without AOT, high surface tension always caused the drops and beaded fibers during electrospinning. So adding surfactant,

TABLE 3 Surface Tension of Electrospinning Solutions at 20 °C

Sample Code	Surface Tension (mN/m)
PNN-fb	28.3
PDPNN4-fb	28.8
PDPNN12-fb	29.8
PDPNN20-fb	30.1
8 wt % of PNN aqueous solution	42.1
PEDOT:PSS solution	63.9
Water	72.0

AOT, was an effective way to lower the surface tension for electrospinning in aqueous system. SEM images of electrospun fibers of PNN-fb, PDPNN4-fb, PDPNN12-fb, and PDPNN20-fb were shown in Figure 3. The diameter of fibers increased obviously when PDEOT:PSS content increased. That was mainly caused by the viscosity of electrospinning solutions. The viscosity of them at various shear rates was shown in Figure 4. When the content of PEDOT:PSS increased, the viscosity also increased, because some physical interaction between PEDOT:PSS and PNN in the solutions caused the increase of frictional force during rheology test. In electrospinning process, the high viscosity retarded the elongation of electrospun fibers, so that higher viscosity always leads to a larger diameter.

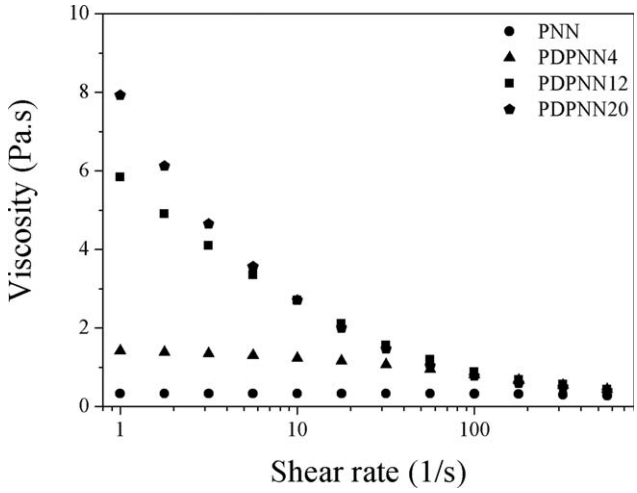

FIGURE 4 Viscosities of electrospinning solutions under various shear rates.

Gel Fraction of TCCs

For fabricating the stable TCC hydrogel, thermocrosslinkable copolymer PNN was synthesized.[17] The crosslinking mechanism was illustrated in Scheme 1. After thermocrosslinking at 110 °C for 12 hr, the stability of TCC films and fiber mats in water was measured by using gel fraction and the result was shown in Table 4. The gel fractions of PNN and PDPNN-20 films were 81.9 and 99.5%, respectively, and those of PNN and PDPNN-20 fiber mats were 57.7 and 96.2%, respectively. The introduction of PEDOT:PSS in the composite efficiently increased the stability of composite. Comparing the structure difference, the dense structure of film showed better stability than the fibrous structure of fiber mats. The increasing of stability might be from the strong hydrogen bonding between amide groups and sulfonic groups on PNN

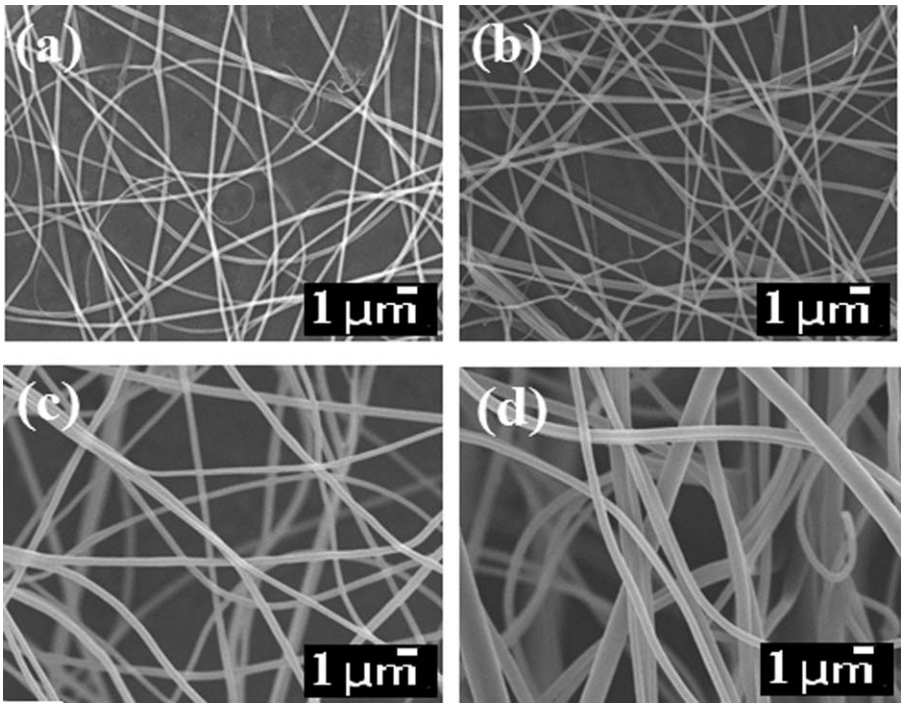

FIGURE 3 SEM images of (a) PNN-fb, (b) PDPNN4-fb, (c) PDPNN12-fb, and (d) PDPNN20-fb.

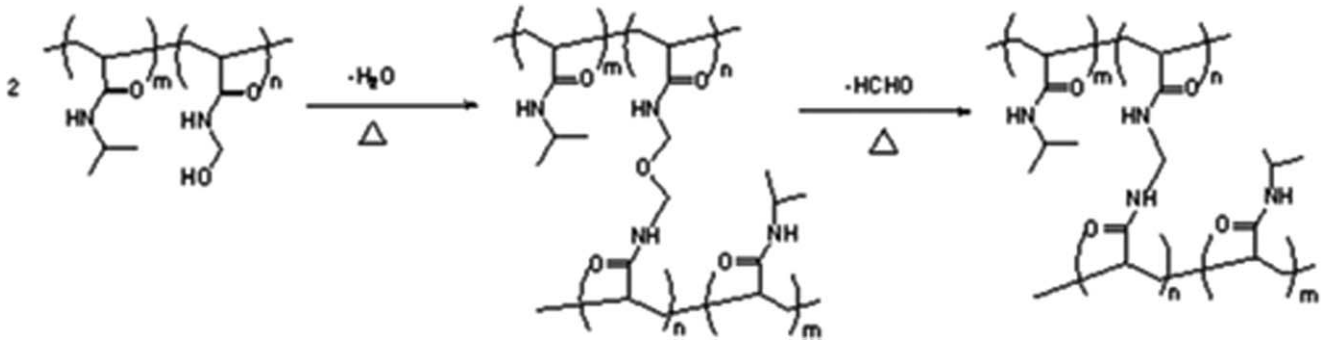

SCHEME 1 Schematic illustration of crosslinking reaction of PNN.

TABLE 4 Gel Fractions of TCC Films and Fiber Mats

Sample	Film	Fiber Mat
PNN	81.9%	57.7%
PDPNN4	93.4%	70.8%
PDPNN12	97.5%	78.4%
PDPNN20	99.5%	96.2%

and PSS. This strong interaction caused the increase of crosslinking density as well as gel fraction.

Phase Transition Behavior (LCST) of TCCs

The thermoresponsive property of TCC films and fiber mats was measured by DSC and the results were shown in Figure 5. For those film samples (*a*, *b*, *c*), PNN showed the obvious endothermic peak owing to the phase transition. When the PEDOT:PSS content was increased to 4 wt %, the peak became broader and slightly shifted to a lower temperature. When the PEDOT:PSS content reached 12 wt % or over, the peak almost vanished. The same trend was also found in the TCC fiber mats (*d*, *e*, *f*). Comparing the crosslinked PNN film and fiber mat with 5 wt % solution (*a*, *d*, *g*), PNN solution showed greater endothermic peak obviously. In other words, the crosslinking process of PNN resulted in the decreasing part of thermoresponsivity. During the phase transition from swelling to shrinking, PNIPAAm segments in PNN aggregated and excluded water from hydrogel. The hydrogen bonding between PNN and water was broken and polymer–polymer and water–water interactions were formed

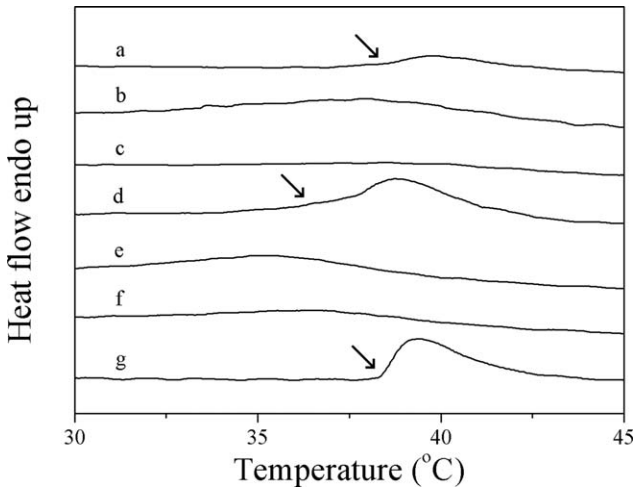

FIGURE 5 DSC diagrams of (a) PNN film, (b) PDPNN-4 film, (c) PDPNN-12 film, (d) PNN fiber mat, (e) PDPNN-4 fiber mat (f) PDPNN-12 fiber mat, and (g) 5 wt % of PNN solution heated from 25 to 45 °C.

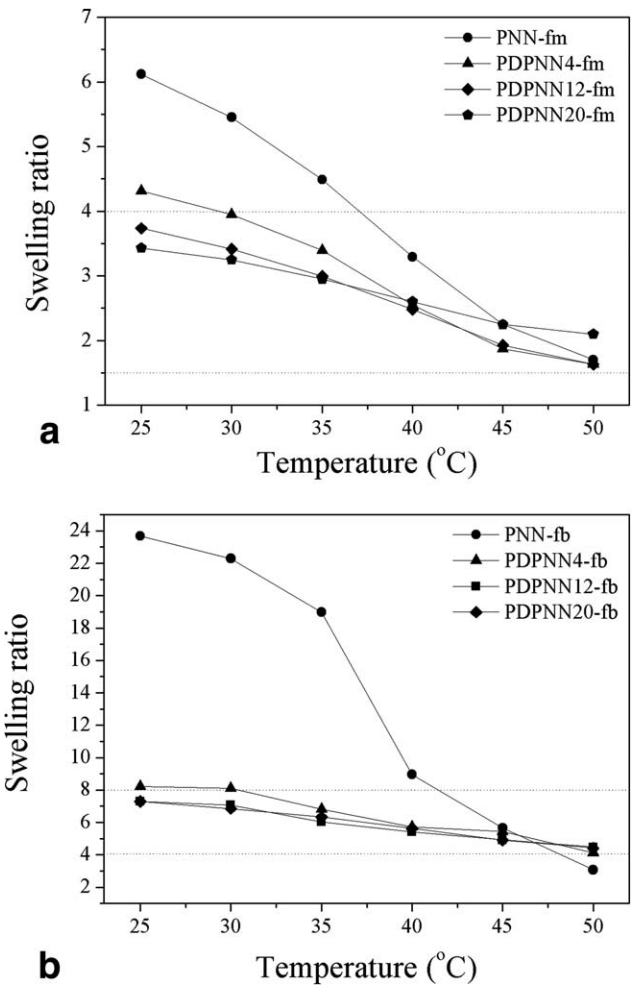

FIGURE 6 Swelling ratio of TCC films and fiber mats under various temperatures (a) TCC films, (b) TCC fiber mats.

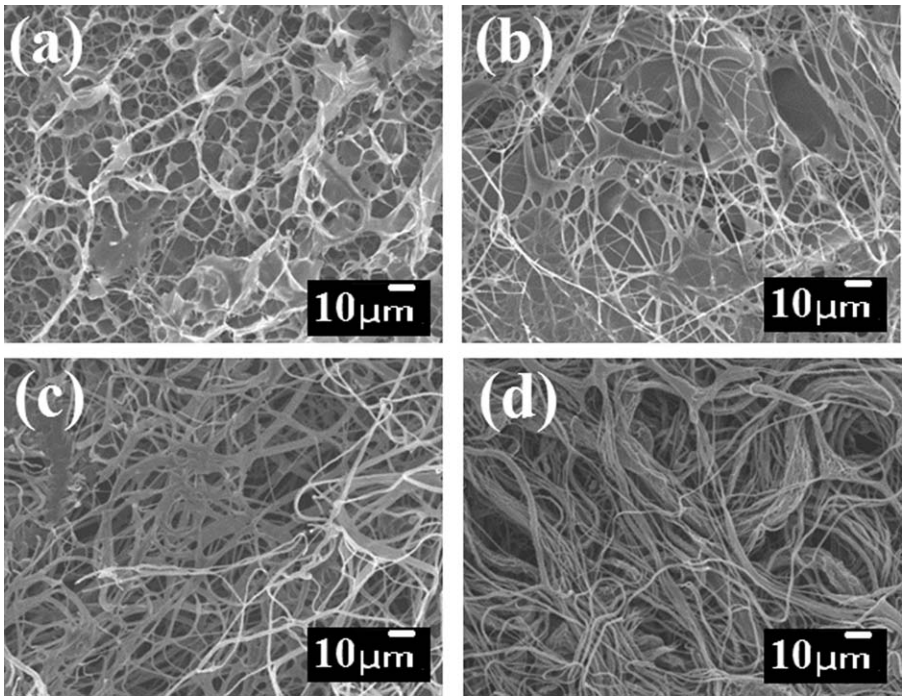

FIGURE 7 SEM images of swollen-dried (a) PNN, (b) PDPNN4, (c) PDPNN12, (d) PDPNN20 fiber mats.

during the phase transition, so the energy difference caused endothermic peak. For PDPNN samples, the incorporation of PEDOT:PSS not only hindered PNN from aggregation during phase transition but also reduced the content of PNN in the hydrogel. So that the endothermic peak of PDPNN showed smaller and broader. Comparing PNIPAAm and PNN solutions, their LCSTs were near 32 and 37 °C, respectively. The incorporation of NMA in the copolymer PNN led LCST to shift to higher temperature. NMA was a hydrophilic monomer which interacted with water by hydrogen bonding, so that phase transition temperature shifted to higher temperature. After the thermocrosslinking of PNN film and fiber mat, hydrophilic NMA groups in the copolymer were consumed to carry on crosslinking reaction. In addition, the concentrations of PNN were locally different in the hydrogel. In high concentration region, the LCST decreased gradually. In low concentration region, the LCST retained like dilute solution.[27,28] In the result, endothermic peak of composite hydrogel shifted to lower temperature and became broader.

Swelling Ratio

Water absorption ability of TCCs under various temperatures, was done by swelling ratio test, and the results were shown in Figure 6. In the swelling ratio test, thermoresponsive composites changed their structure from swelling to shrinking during heating. During the phase transition, water in the gels was expelled from thermoresponsive composites, and the total weight of composites reduced gradually. For TCC films and fiber mats, the incorporation of PEDOT:PSS in the composite led to not only the decrease of swelling ratio at temperature below LCST but also the reduction of the swelling ratio difference during phase transition. Comparing the structure between fiber mats and film, fiber mats showed greater water-absorption ability than films below and above LCST. For TCCs, PEDOT:PSS and PNN polymer chains interpenetrated each other. At temperature below LCST, hydrophobic PEDOT chains blocked the sites and that could absorb water in TCCs. In addition, PDPNN composites with high crosslinking density also led to decrease of water-absorption ability. During the phase transition from hydrophilicity to hydrophobicity, PEDOT:PSS chains hindered PNN from aggregation. Incomplete shrinking caused the decrease of thermoresponsivity. In the test of fiber mats, some water was trapped in the network of fiber mat. So, at temperatures below and above LCST, the swelling ratios of PNN-fb and PDPNN-fb were higher than those of films. Extra high swelling ratio of PNN-fb might be caused by relatively low crosslinking density (Table 4), and that made hydrogel to expand easily. Comparing TCC films and fiber mats, the swelling of films and fiber mats were changed from about 4 to 1.5 and 8 to 4, respectively. The higher difference of swelling ratio of TCC fiber mats than films was found, because fibrous structure can change its structure easier and faster than the dense structure.

To realize the structural change of fiber mats during phase transition, the morphology of swollen-dried and shrunk-dried composite fiber mats was observed by SEM as shown in Figures 7 and 8, respectively. In Figure 7, because of good water-absorption ability below LCST, high porosity of swelling-dried fiber mats could be observed. When the content of PEDOT:PSS increased, the integrity of fiber mats was improved, due to the increase of gel fraction. Under the shrinking condition as shown in Figure 8, porous structure was still found in PDPNN fiber mats, because PEDOT:PSS in

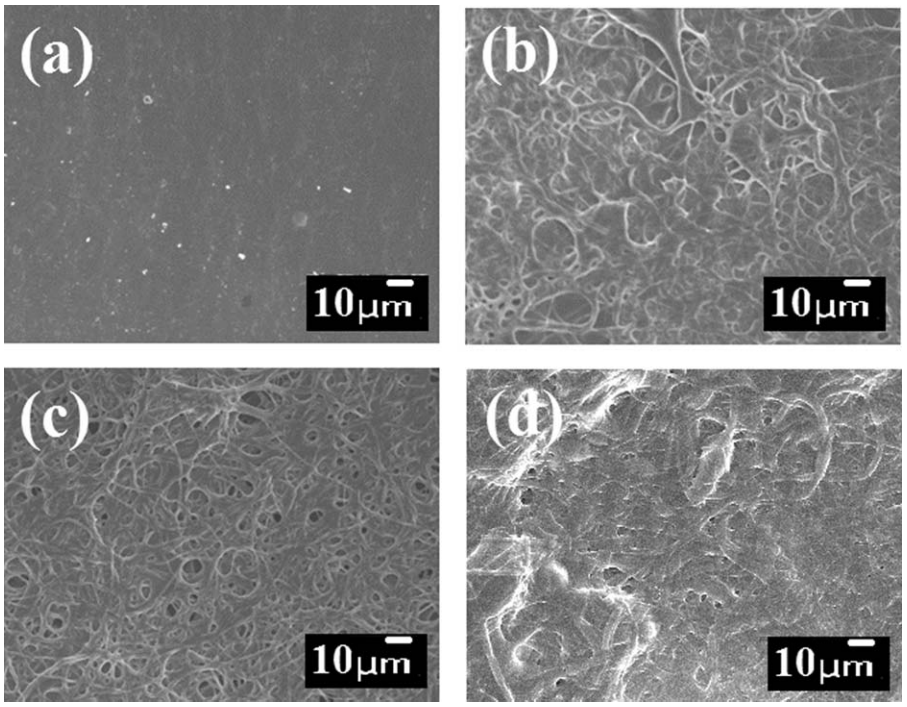

FIGURE 8 SEM images of shrunk-dried (a) PNN, (b) PDPNN4, (c) PDPNN12, (d) PDPNN20 fiber mats.

the PDPNN fibers confined the motion of network during the phase transition. On the other hand, dense structure was observed in PNN sample, because PNN chains could move more freely during shrinking. That is also the main reason for the extra high swelling ratio difference between below and above LCST for PNN fiber mats.

Electrical Properties of TCCs

The other important property, electrical property, of TCC thin films and fiber mats were measured by voltmeter and calculated using eq 3. The surface resistance, film thickness, and conductivity of TCCs were shown in Table 5 and Figure 9. Conductivity of TCCs increased with PEDOT:PSS content, because PEDOT was served as the conductive component in the composite, and the increase of PEDOT content led conductive PEDOT to form more continuous tunnels. Comparing TCC thin films with fiber mats, the conductivity of thin films were greater than that of fiber mats at the same PEDOT:PSS content. Fibrous structure which had voids and boundaries in the material reduced the electron transporting rates, so this structural difference resulted in the decrease of conductivity.

TABLE 5 Electric Properties of TCC Thin Films and Fiber Mats

Sample Code	Surface Resistance (Ω/□)	Film Thickness (μm)	Conductivity (S/cm)
PDPNN4-fm	136,400	0.879	0.084
PDPNN8-fm	11,366	0.836	1.05
PDPNN12-fm	675	0.831	17.8
PDPNN16-fm	140	0.844	84.6
PDPNN20-fm	61.6	0.844	192.3
PDPNN4-fb	33,300	3.52	0.085
PDPNN8-fb	5,265	3.80	0.499
PDPNN12-fb	648.8	3.56	4.3
PDPNN16-fb	511.5	3.04	6.9
PDPNN20-fb	279.3	3.19	11.2

Thermoresponsive Conductive Property of TCCs

To study the temperature effect on electric property of TCCs, TCC electrodes which connected to voltmeter were immersed in water bath under various temperatures from 25 to 50 °C. After TCCs swelled in water, their surface resistance increased, because the water which penetrated into the

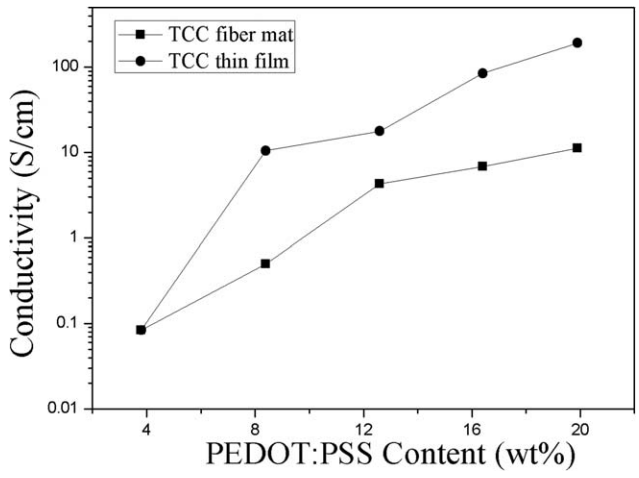

FIGURE 9 Conductivities of TCC thin films and fiber mat with various PEDOT:PSS content.

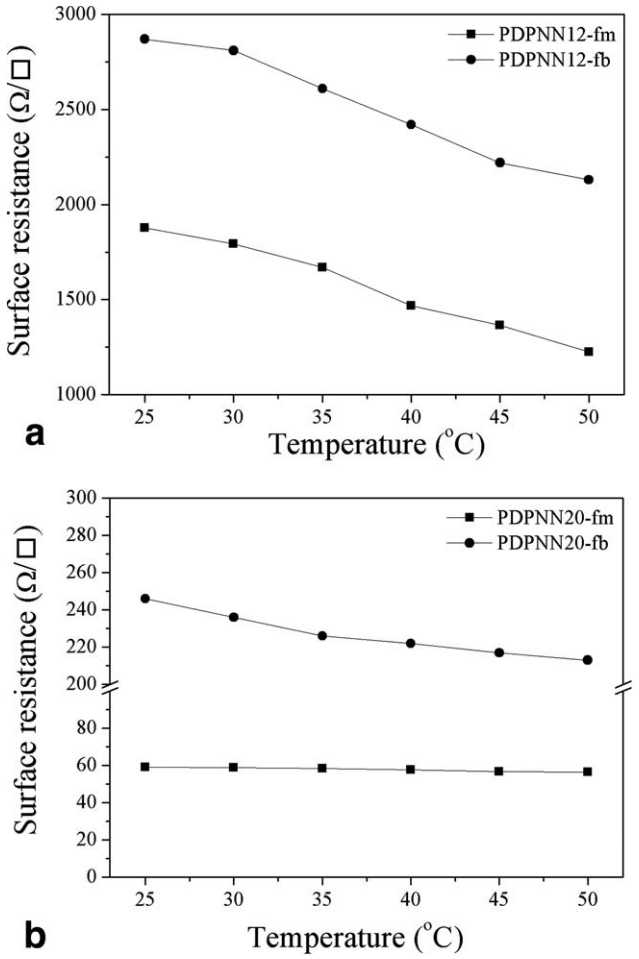

FIGURE 10 Surface resistances of (a) PDPNN12 film and fiber mat, (b) PDPNN20 film and fiber mat under various temperatures.

TCCs loosened the structure and retarded the electron transport. The surface resistance of PDPNN4 thin films and fiber mats were too high (~MΩ/□) owing to the large amount of penetrated water, so we focused on TCCs with low resistance (less than 10 kΩ/□). The surface resistances of TCC electrodes under various temperatures were shown in Figure 10. The surface resistance of TCCs exhibited thermoresponsivity and decreased gradually with temperature. PDPNN12 thin film and fiber mat exhibited greater difference of surface resistance than PDPNN20 samples. For the same content of PEDOT:PSS samples, TCCs with fibrous structure showed greater difference of surface resistance during heating. In other words, PDPNN12 fiber mats can provide great thermosensitivity. During the heating of TCCs, TCCs gradually changed from swelling hydrogel to shrinking rubber-like material, and the penetrated water was expelled from TCCs. The shrinking increased the continuity of conductive PEDOT:PSS domains in TCCs, so the lowering of surface resistance with the increasing of temperature was observed. In the swelling ratio test and LCST measurement, we realized thermoresponsivity decreased with increasing the content of PEDOT:PSS. So PDPNN12 samples showed greater difference of surface resistance than PDPNN20 samples. Comparing the structural difference, the greater difference of surface resistance for fiber mats was due to the larger structural change during phase transition. In the result, PDPNN12 fiber mat with fibrous structure performed the best thermoresponsive conductive property among all TCC samples.

CONCLUSION

We synthesized thermoresponsive copolymer, PNN, with thermocrosslinking ability successfully. By the combination of PNN and PEDOT:PSS, thermoresponsive conductive composite thin films, and fiber mats were fabricated using spin-coating and electrospinning technique. During electrospinning process in water system, surfactant, AOT, reduced the surface tension of electrospinning solutions and prevented from the formation of beaded fibers. When the content of PEDOT:PSS increased in the composites, the gel fraction of films, and fiber mats increased because of the interaction between PEDOT:PSS and PNN, but the thermoresponsivity gradually decreased. On the contrary, conductivity of TCCs was improved with increasing the content of PEDOT:PSS owing to the better continuity of conductive domains. In the thermoresponsive conductive property experiment, TCC thin films and fiber mats exhibited their thermoresponsivity by changing the surface resistance. PDPNN12 fiber mat with fibrous structure performed the best thermoresponsive conductive property. This fiber mat could be used as thermosensor applications.

REFERENCES AND NOTES

1 J. Hu, H. Meng, G. Li, S. I. Ibekwe, *Smart Mater. Struct.* **2012**, *21*, 053001.

2 B. Jeong, A. Gutowska, *Trends Biotechnol.* **2002**, *20*, 305–311.

3 R. Gomes de Azevedo, L. P. N. Rebelo, A. M. Ramos, J. Szydlowski, H. C. de Sousa, J. Klein, *Fluid Phase Equilib.* **2001**, *185*, 189–198.

4 J. T. Zhang, S. Petersen, M. Thunga, E. Leipold, R. Weidisch, X. Liu, A. Fahr, K. D. Jandt, *Acta Biomater.* **2010**, *6*, 1297–1306.

5 X. Z. Zhang, D. Q. Wu, C. C. Chu, *Biomaterials* **2004**, *25*, 3793–3805.

6 X. Lu, C. Wang, Y. Wei, *Small* **2009**, *5*, 2349–2370.

7 D. Aussawasathien, C. Teerawattananon, A. Vongachariya, *J. Membr. Sci.* **2008**, *315*, 11–19.

8 X. Wang, F. Cui, J. Lin, B. Ding, J. Yu, S. S. Al-Deyab, *Sens. Actuators B: Chem.* **2012**, *171172*, 658–665.

9 B. Ding, M. Yamazaki, S. Shiratori, *Sens. Actuators B: Chem.* **2005**, *106*, 477–483.

10 Z. Ma, M. Kotaki, R. Inai, S. Ramakrishna, *Tissue Eng.* **2005**, *11*, 101–109.

11 J. P. Chen, G. Y. Chang, J. K. Chen, *Colloids Surf. Physicochem. Eng. Aspects* **2008**, *313314*, 183–188.

12 W. A. Daoud, J. H. Xin, Y. S. Szeto, *Sens. Actuators B: Chem.* **2005**, *109*, 329–333.

13 A. Laforgue, L. Robitaille, *Synth. Met.* **2008**, *158*, 577–584.

14 A. Laforgue, L. Robitaille, *Macromolecules* **2010**, *43*, 4194–4200.

15 N. Liu, G. Fang, J. Wan, H. Zhou, H. Long, X. Zhao, *J. Mater. Chem.* **2011**, *21*, 18962.

16 O. Martínez, A. G. Bravo, N. J. Pinto, *Macromolecules* **2009**, *42*, 7924–7929.

17 W. J. Chuang, W. Y. Chiu, H. J. Tai, *Mater. Chem. Phys.* **2012**, *134*, 1208–1213.

18 H. Wang, J. Zheng, M. Peng, *J. Appl. Polym. Sci.* **2010**, *115*, 2485–2492.

19 S. S. Choi, J. P. Hong, Y. S. Seo, S. M. Chung, C. Nah, *J. Appl. Polym. Sci.* **2006**, *101*, 2333–2337.

20 Z. Tang, J. Wei, L. Yung, B. Ji, H. Ma, C. Qiu, K. Yoon, F. Wan, D. Fang, B. S. Hsiao, B. Chu, *J. Membr. Sci.* **2009**, *328*, 1–5.

21 Y. Z. Zhang, J. Venugopal, Z. M. Huang, C. T. Lim, S. Ramakrishna, *Polymer* **2006**, *47*, 2911–2917.

22 C. Yao, X. Li, T. Song, *J. Appl. Polym. Sci.* **2007**, *103*, 380–385.

23 Y. Jin, D. Yang, Y. Zhou, G. Ma, J. Nie, *J. Appl. Polym. Sci.* **2008**, *109*, 3337–3343.

24 H. E. Yin, C. F. Lee, W. Y. Chiu, *Polymer* **2011**, *52*, 5065–5074.

25 Y. Jung, H. Kim, D. Lee, S. Park, M. Khil, *Macromol. Res.* **2005**, *13*, 385–390.

26 L. Yao, T. W. Haas, A. Guiseppi-Elie, G. L. Bowlin, D. G. Simpson, G. E. Wnek, *Chem. Mater.* **2003**, *15*, 1860–1864.

27 C. S. Brazel, N. A. Peppas, *Macromolecules* **1995**, *28*, 8016–8020.

28 Z. Tong, F. Zeng, X. Zheng, T. Sato, *Macromolecules* **1999**, *32*, 4488–4490.